Transportation Research Part B 96 (2017) 46–67

Contents lists available at ScienceDirect

Transportation Research Part B

journal homepage: www.elsevier.com/locate/trb

# Multiperiod-based timetable optimization for metro transit networks

Xin Guo[a,b,c], Huijun Sun[b,*], Jianjun Wu[a,*], Jiangang Jin[d], Jin Zhou[b], Ziyou Gao[b]

[a] State Key Laboratory of Rail Traffic Control and Safety, Beijing Jiaotong University, Beijing 100044, China
[b] School of Traffic and Transportation, Beijing Jiaotong University, Beijing 100044, China
[c] Department of Civil and Environmental Engineering, University of Wisconsin-Madison, Madison, WI 53706, USA
[d] School of Naval Architecture, Ocean and Civil Engineering, Shanghai Jiao Tong University, Shanghai, 200240, China

ARTICLE INFO

*Article history:*
Received 16 March 2016
Revised 1 November 2016
Accepted 1 November 2016
Available online 19 November 2016

*Keywords:*
Multiperiod
Metro transit network
Transfer synchronization

ABSTRACT

This paper tackles the train timetable optimization problem for metro transit networks (MTN) in order to enhance the performance of transfer synchronization between different rail lines. Train timetables of connecting lines are adjusted in such a way that train arrivals at transfer stations can be well synchronized. This study particularly focuses on the timetable optimization problem in the transitional period (from peak to off-peak hours or vice versa) during which train headway changes and passenger travel demand varies significantly. A mixed integer nonlinear programming model is proposed to generate an optimal train timetable and maximize the transfer synchronization events. Secondly, an efficient hybrid optimization algorithm based on the Particle Swarm Optimization and Simulated Annealing (PSO-SA) is designed to obtain near-optimal solutions in an efficient way. Meanwhile, in order to demonstrate the effectiveness of the proposed method, the results of numerical example solved by PSO-SA are compared with a branch-and-bound method and other heuristic algorithms. Finally, a real-world case study based on the Beijing metro network and travel demand is conducted to validate the proposed timetabling model. Computational results demonstrate the effectiveness of adjusting train timetables and the applicability of the developed approach to real-world metro networks.



## 1. Introduction

As the most reliable and energy efficient transportation system, metro transit has been developed as a solution to mitigate road congestion and associated environmental pollutions, and thus plays an increasingly important role in many large cities over the world (Kang et al., 2015a). Due to the large scale of the network, the design of metro transit is often addressed into two stages, tactical planning and operational management. Various decision-making problems arise accordingly, such as line planning, timetable generation, vehicle scheduling, and crew scheduling (Ceder, 2007; Ibarra-Rojas and Rios-Solis, 2012; Yang et al., 2013; Yang et al., 2016). As one critical challenge in the planning stage, timetable design affects, to a significant extent, the service quality as well as those subsequent planning problems including path and crew scheduling.

Transfer synchronization of different train lines affects the service quality to a large extent. In addition to travel time on trains, the maximal transfer synchronization time of different trains will be just close to headway in the peak period,

* Corresponding authors.
*E-mail addresses:* hjsun1@bjtu.edu.cn (H. Sun), jjwu1@bjtu.edu.cn (J. Wu).

http://dx.doi.org/10.1016/j.trb.2016.11.005
0191-2615/

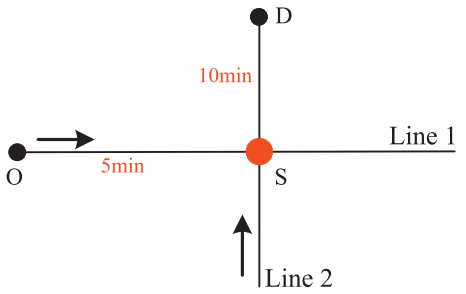


**Fig. 1.** Illustration of a small network.

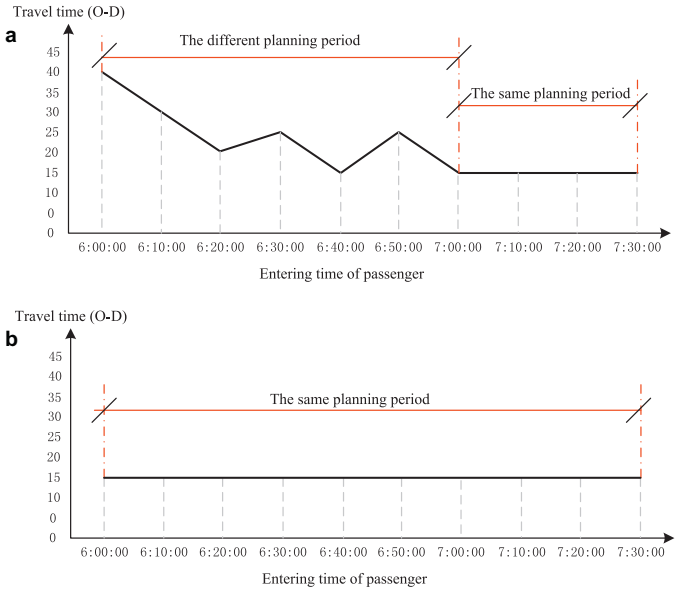


**Fig. 2.** (a) A snapshot of small metro network. (b) A snapshot of small metro network.

**Table 1**
The headways in different time periods.

| | | | | |
|---|---|---|---|---|
| Line 1 | Departure time of first train | | 06:00:00 | |
| | Time period | 06:00:00–07:00:00 | | 07:00:00–07:30:00 |
| | Headway (min) | 20 | | 10 |
| Line 2 | Departure time of first train | | 06:30:00 | |
| | Time period | 06:30:00–07:00:00 | | 07:00:00–08:00:00 |
| | Headway (min) | 15 | | 5 |

Note: The time is represented in the 24-h HH:MM:SS format.

because frequencies tend to be high and missing a connection only increases passengers' transfer waiting time by a relatively short interval (Chakroborty, 2003). In contrast, for those who make transfers through different lines during the off-peak period, when service frequency is low, passengers may spend additional time waiting for train services. Moreover, considering the varied travel demand of an entire day, rail operators commonly adjust timetables and change headways from period to period, e.g., the first train period, the morning peak period, the morning off-peak period, the afternoon peak period, the afternoon off-peak period and the last train period. For a metro transit network (MTN) which is operated by multiple rail operators, different operating strategies may be adopted for different lines. Inappropriate synchronization of train services in different lines during the transitional period (from peak to off-peak hours or vice versa) may lead to an unacceptable amount of waiting time for passengers. Therefore, it is necessary to enhance the transfer synchronization between different rail lines.

We use a small network to illustrate this problem (see Figs. 1 and 2). In Fig. 1, there is an OD (origin to destination) pair and a transfer station *S*. Running directions are denoted by arrows and the running time is marked in red. The initial departure time and headways in various periods are provided in Table 1. Assume that the walking time and boarding time equal to zero.

**Table 2**
The travel time for various time periods.

| Departure time | | | | Arrival time at D | Travel time (min) |
|---|---|---|---|---|---|
| O | Train of Line 1 at O | S | Train of Line 2 at S | | |
| 6:00:00 | 6:00:00 | 6:05:00 | 6:30:00 | 6:40:00 | **40** |
| 6:10:00 | 6:20:00 | 6:25:00 | 6:30:00 | 6:40:00 | **30** |
| 6:20:00 | 6:20:00 | 6:25:00 | 6:30:00 | 6:40:00 | **20** |
| 6:30:00 | 6:40:00 | 6:45:00 | 6:45:00 | 6:55:00 | **25** |
| 6:40:00 | 6:40:00 | 6:45:00 | 6:45:00 | 6:55:00 | **15** |
| 6:50:00 | 7:00:00 | 7:05:00 | 7:05:00 | 7:15:00 | **25** |
| 7:00:00 | 7:00:00 | 7:05:00 | 7:05:00 | 7:15:00 | 15 |
| 7:10:00 | 7:10:00 | 7:15:00 | 7:15:00 | 7:25:00 | 15 |
| 7:20:00 | 7:20:00 | 7:25:00 | 7:25:00 | 7:35:00 | 15 |
| 7:30:00 | 7:30:00 | 7:35:00 | 7:35:00 | 7:45:00 | 15 |

Note: The time is represented in the 24-h HH:MM:SS format.

A passenger entry station O at 6:00:00 am, and one can take the train of Line 1 whose departure time is 6:00:00 am at O, and then one can take the train of Line 2 at 6:30:00 am to destination D. Table 2 and Fig. 2a illustrate that the various time periods among different lines may change the travel time in MTN. In the same planning period, travel time keeps stable for different entry time of passengers (See Fig. 2b). Thus, synchronization of transfers in the transitional period should be taken into account in timetabling.

It is a common practice that metro transit operates according to a fixed headway during the peak and off-peak period, while train schedule should be determined carefully considering of the high variability of demand in the transitional period. Thus control strategies pone to variable headways should be applied to avoid inappropriate coordination and capture the maximal synchronization. To show this problem clearly, Fig. 3 illustrates three types of synchronization:

(1) In type 1, all trains in two lines are all synchronized well. Passengers in line $l$ can smoothly transfer to line $l$'.
(2) In type 2, although passengers from train $q-1$ of line $l$ can ride on the trains $q'-1$, $q'$, $q'+1$ and $q'+2$ of line $l$', passengers would like to leave with the first arriving train. Thus, valid coordination would be occurred between trains $q$ and $q'-1$, or trains $q$ and $q'$.
(3) In type 3, train $q$ and $q-1$ are defined as invalid coordination with train $q'$, due to an overlong synchronization time for passengers to transfer.

In contrast to the peak period, we focus on enhancing inappropriate synchronization of train services in the transitional period, instead of oversaturated conditions to ease congestion. Actual data of Beijing metro are utilized to validate the rationality. Here, the maximum passenger volume which along with different periods in key lines are illustrated in Fig. 4. In line 1, a total of 36,500 passengers passed through the section (Dawanglu to Guomao) from 08:00 to 09:00 denoted by the blue bar. The number of passengers has overwhelmed the capacity denoted by a red dot. The histogram reveals that the oversaturated condition often occurs in the peak period (i.e., 08:00–09:00 in Beijing metro). However, in other periods, the train capacity is sufficient.

Because of the inherent uncertainties in MTN, passengers prefer a flexible transfer rather than an instant one. Therefore, the definition of synchronization is the arrival of two trains at a transfer station with a separation time within a small time window instead of simultaneous arrivals. Therefore, in order to finish the transfer smoothly from the peak period to the off-peak period or from the off-peak period to the peak period, a multiperiod transitional timetable model is proposed in this paper.

The remainder is organized as follows. We present a literature review in Section 2. The proposed formulation is presented in Section 3. In Section 4, a branch-and-bound method is adopted to obtain the optimal solution for the numerical experiment. However, due to the NP-hardness complexity of the proposed model, we develop a time-saving hybrid algorithm: PSO-SA, based on the preprocessing stage to solve the Beijing metro network in Section 5. Finally, Section 6 summarizes the results and suggestion in the further.

## 2. Literature review

Metro timetable optimization involves designing a timetable for which trade-offs are made between travelers who want short waiting times as the frequencies tend to be high and operators who want to minimize operational costs via reducing trains. Thus, different measures are built to solve metro timetable problems specifically with a certain optimization period (i.e., the first train period, the last train period, the peak period, the off-peak period and the transitional period). In each period, timetable problems focus on finding an optimal solution to achieve a certain goal, such as decreasing waiting time, reducing operational or travel costs, improving accessibility and increasing synchronization events (Tong et al., 2015), etc.

In the peak period, the traditional accessibility measures are based on travel time or transfer waiting time to improve service levels, due to insufficient capacity and oversaturated conditions. There are many researches optimized the timetable

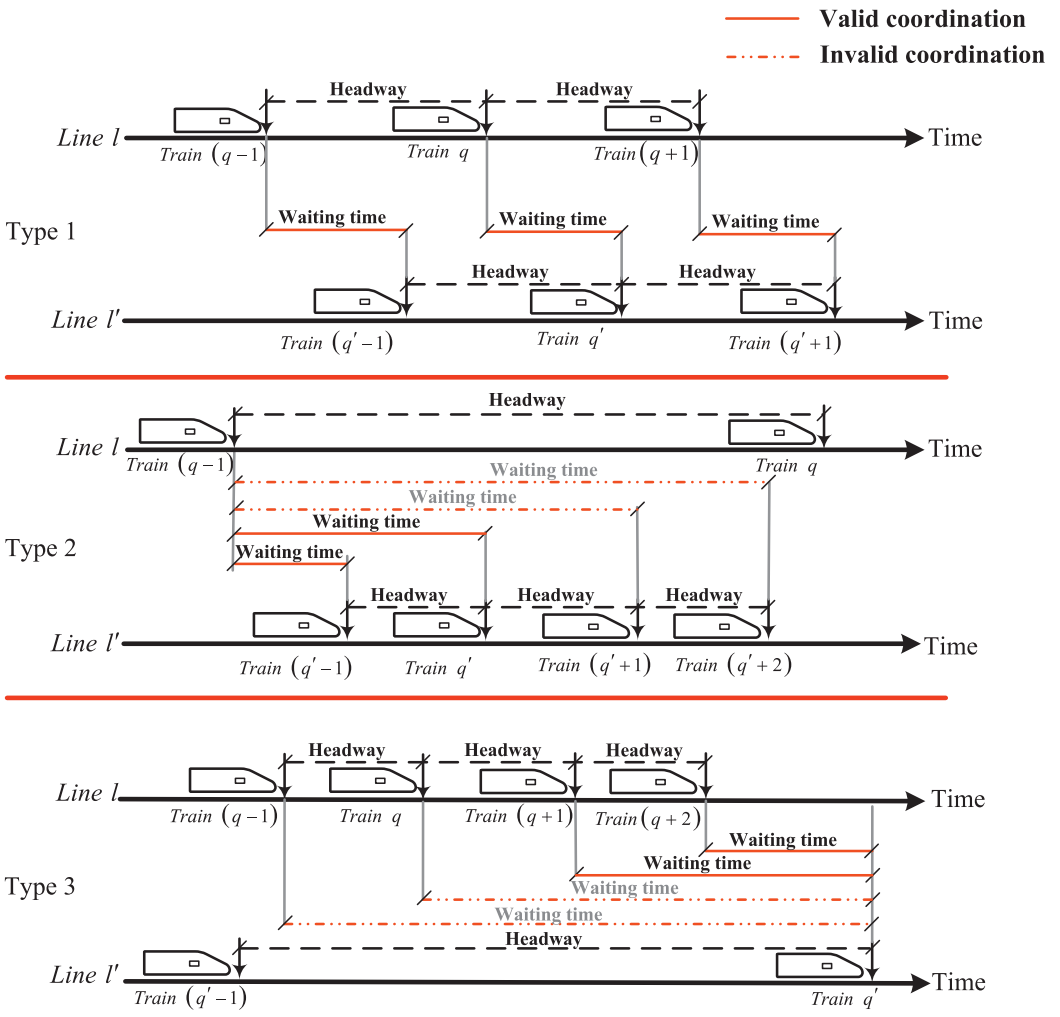


**Fig. 3.** The types of coordination.

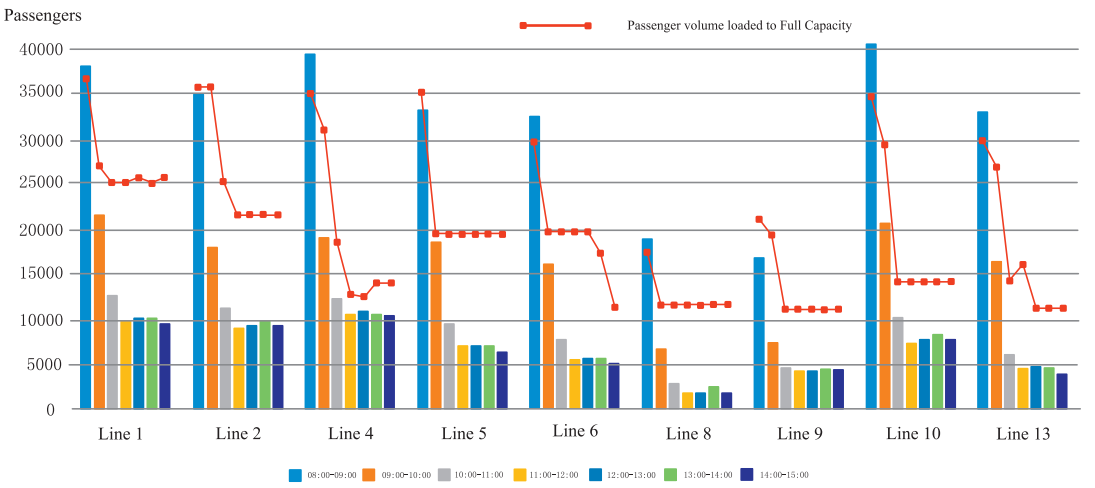


**Fig. 4.** Maximum passenger volume of one section in Beijing metro lines.

by minimizing passenger travel time or transfer time at railway stations, which have been reviewed as Vaughan (1986), Domschke (1989), Nachtigall and Voget (1997), Odijk (1996), Wong and Leung (2004), Cevallos and Zhao (2006), Wong et al. (2008), Liebchen (2008), Shafahi and Khani (2010) and Sels et al. (2016). For example, Wong et al. (2008) developed a mixed integer programming optimization model to minimize all passengers' transfer waiting time in MTN. Liebchen (2008) optimized the arrival and departure times at transfer stations of the Berlin metro network so that passengers' transfer time between the lines were minimized. Shafahi and Khani (2010) proposed two mixed integer programming (MIP) models which could give the departure times of vehicles in lines and aimed to minimize the waiting time at transfer stations. Sels et al. (2016) derived a PESP model to minimize the total passengers' travel time in cyclic timetabling, and macroscopic simulations is utilized to generate a robust railway timetable. Moreover, minimizing the maximal waiting time is the other type of the modified objective for this approach. This objective was based on the assumption of preventing extremely long waiting time for transferring passengers (Daduna and Voß, 1995; Wu et al., 2015). Meanwhile, optimization models aimed at minimizing the generalized cost to design the optimal timetable have been proposed by Yan and Chen (2002), Lin and Chen (2008), Gallo et al. (2011), Kou et al. (2014) and Yang et al. (2015). Combining with these two objectives: minimizing passengers' waiting time and generalized costs have been studied by Chang et al. (2000), Castelli et al. (2004), Ibarra-Rojas and Rios-Solis (2012) and Yang et al. (2014).

Recently, other researchers tend to place more emphasis on the consideration of travel demand, transfer space-time accessibility and oversaturated conditions to ease congestion. To create an efficient timetable related to passenger demand, Ceder (2007) created timetables with balanced passenger volumes using the settled rate of passenger arrivals in small time periods. Palma and Lindsey (2001) assumed that each passenger has an ideal boarding time and incurs a varying schedule delay cost from traveling earlier or later. Ceder et al. (2013) minimized the deviation from the desired passenger volume while trying to maintain even headways using buses with different sizes. Mesa et al. (2014) proposed a mathematical formulation based on the q-median problem to minimize the passenger's inconvenience considering the constraints of limited number of trips, limited fleet size, and limited vehicles' capacities. Moreover, Kang et al. (2013) proposed an activity-based network design problem, which focused more on tactical policies, rather than on operational technologies and real-time flow. Then Kang and Chen (2016) continued to propose a household activity pattern problem to obtain the feasible region in the space–time dimension based on definitions and constraints on this model. In addition, Tong et al. (2015) addressed a new urban network by maximizing transportation accessibility between major activity locations path through a space–time analysis network. To ease congestion, Niu et al. (2015) proposed a timetabling model for two interconnected lines is to balance passenger waiting times at stations and in-train crowding disutility at transfer stations under time-dependent demand conditions so that transfer passengers can arrive at their destinations quickly and conveniently.

The synchronization issue between different lines is a critical issue affecting passengers' waiting time due to the relatively lower service frequency during off-peak period (see reviews of Desaulniers and Hickman, 2007; Guihaire and Hao, 2008; Ibarra-Rojas et al., 2015b). To improve transfer mobility, Ceder et al. (2001) focused on maximizing the number of pairwise simultaneous arrivals at stations in order to benefit passenger transfers. Albrecht and Oettich (2002) proposed an algorithm for the dynamic modification of train running time to increase the probability of making connections to other means of public transport. Eranki (2004) extended the definition of synchronization which is presented in Ceder et al. (2001). Synchronization is redefined as the arrival of two trips at a station with a separation time within a small time window instead of simultaneous arrivals. Fleurent et al. (2004) described the concepts that were implemented in commercial software Hastus to generate synchronized transit timetables. A global synchronization quality index was also defined to measure the quality of synchronization for the entire network. Cevallos and Zhao (2006) used the genetic algorithm (GA) to optimize an existing timetable to increase coordination between lines. Ibarra-Rojas and Rios-Solis (2012) proposed a mixed integer linear formulation to redefine a synchronization event. These synchronization events are utilized to benefit passenger transfers and to reduce bus congestion at stations. Wu et al. (2016) investigated a multi-objective re-synchronizing of the bus timetable to adjust the original bus timetable in order to benefit more passengers by synchronizing bus arrival times at transfer stations.

Scheduling the first and last trains has been gaining research interests recently. The main purpose is to minimize of passenger inconvenience (usually measured by waiting time) caused by the first/last transfer service. Kang et al. (2015b) constructed a last train optimization model to minimize the running time and dwell time and maximize the average transfer redundant time and network transfer accessibility. Zhou et al. (2013) constructed two coordination optimization models to minimize passengers' total originating waiting time for first trains and transfer waiting time for last trains. Dou et al., (2015) proposed an optimal bus schedule coordination problem for last train service by offsetting and perturbing the original bus schedules to reduce transfer failures from bus service to train service based on the given last train schedules. Guo et al. (2016) proposed a timetable coordination model, based on the importance of lines and transfer stations, to improve the transfer performance in that they reduce the connection time for the first trains in metro networks.

In the transitional period, the synchronizations of crossing metro lines at transfer stations are always ignored. The division of a day into smaller time periods based on demand and travel time variability is not straightforward (Salicrú et al., 2011). Moreover, the divisions are not necessarily the same for different lines. Ibarra-Rojas et al., (2015a) extended the approach of Ibarra-Rojas and Rios-Solis (2012) to consider multiple time periods. The authors defined a synchronization event between trips belonging to different periods as the pair wise arrival at transfer stations. Ibarra-Rojas et al. (2016) then proposed an integer linear programming formulation to maximize the bus service quality and minimize bus bunching along the network.

Although a number of models have been developed for train timetabling, few works focus on the train service synchronization during the transitional time periods as mentioned above. With the development of MTN, it is increasingly urgent to optimize departure times in the transitional period to facilitate passengers' smooth transferring. On the other hand, this multiperiod timetabling problem cannot be solved completely with the general models because the definitions of synchronizations between trains are not the same. The contributions of this paper are given as follows. First, we propose a synchronized train timetabling model with smooth transitions under a given passenger service level. The objective is to maximize the number of synchronization events for MTN during the transitional period. Secondly, a hybrid algorithm, PSO-SA, is designed to solve real-size instances. In addition, the effectiveness of the proposed model and solution approach is validated by showing that merging a single period significantly improves the system synchronization.

## 3. Formulation

This section develops a mixed integer nonlinear programming model to generate the optimal train timetable with the objective of maximizing transfer synchronizations. MTN is defined as a directed graph with transfer stations denoted by nodes and metro lines represented by directed links. The notations of the mathematical formulation are defined as follows:

### 3.1. Symbols

*Parameters*

| | |
|---|---|
| $T$ | set of discrete time periods of the planning horizon, $T \in \{1, 2, 3\ldots\}$; |
| $t$ | index of time, $t \in [T_1, T_2]$, $T_2 - T_1$ is the planning time period; |
| $L$ | set of lines, $l \in L$, $L=\{l \mid l=1, 2\ldots m\}$, where $m$ is the total number of lines in MTN; |
| $S(l)$ | set of transfer stations of line $l$, $s \in S(l)$, $S(l)=\{s \mid s=1, 2\ldots k\}$, where $k$ is the total number of transfer stations of line $l$; |
| $S$ | index of transfer stations, $S(l) \in S$, $S=\{S(l) \mid S(l)=S(1), S(2)\ldots S(m)\}$; |
| $q$ | train in line $l$, $q=1, 2\ldots N_l$, where $N_l$ is the total number of trains in line $l$. Similarly, the train in line $l'$ is denoted by $q'$, and there are $N_{l'}$ trains in line $l'$; |
| $t^T_{ll's}$ | transfer walking time from line $l$ to line $l'$ at transfer station $s$; |
| $h^p_{l,\max}$ | maximum headway of line $l$ in the transitional period; |
| $h^p_{l,\min}$ | minimum headway of line $l$ in the transitional period; |
| $P^H_{lql'q's}(t)$ | number of passengers transferring from train $q$ in line $l$ to train $q'$ in line $l'$ at transfer station $s$ and time $t$, $t \in [T_1, T_2]$. |

*Decision variables*

| | |
|---|---|
| $t^A_{lqs}$ | arrival time of train $q$ at transfer station $s$ in line $l$; |
| $t^D_{lqs}$ | departure time of train $q$ at transfer station $s$ in line $l$; |
| $t^R_{lq(s-1)s}$ | running time of train $q$ in line $l$ from transfer station $(s-1)$ to transfer station $s$; |
| $t^E_{lqs}$ | dwell time of train $q$ at transfer station $s$ in line $l$; |
| $h_{lq}$ | headway of the train $q$ and train $q+1$ line $l$ in the transitional period; |

### 3.2. Assumptions

**Assumption 1.** In the transitional period (non-peak hours), the train capacity is enough to accommodate all passengers. Therefore, passengers will get on the first arriving train.

**Assumption 2.** Passengers are all reasonable in real life and they are assumed more inclined to take the path with less travel time.

**Assumption 3.** The headways in per line are assumed uniform in the peak or off-peak period according to the existing timetable. A periodic timetable provides the most efficient operation. Constant headways may result in better coordination in transfer stations, and a satisfactory transfer can be easily repeated (Kang et al., 2015a; Shafahi and Khani, 2010).

### 3.3. Passenger waiting time and train synchronization time

The passenger waiting time (PWT) can be calculated by Eq. (1) with three cases described in Fig. 5 respectively. Note that PWT is proposed to find synchronization events via differentiating with train synchronization time.

In case 1, passengers from the train $q$ in line $l$ can ride the train $q'$ in line $l'$ successfully; the PWT is greater than zero and less than the headway. It is equal to the departure time of the train $q'$ in line $l'$ at transfer station $s$ minus the arrival time of the train $q$ in line $l$ at transfer station $s$, minus transfer walking time between line $l'$ and line $l$; in case 2, the waiting time between train $q$ in line $l$ and train $q'+H$ in line $l'$, which equals to the waiting time between train $q$ in line $l$

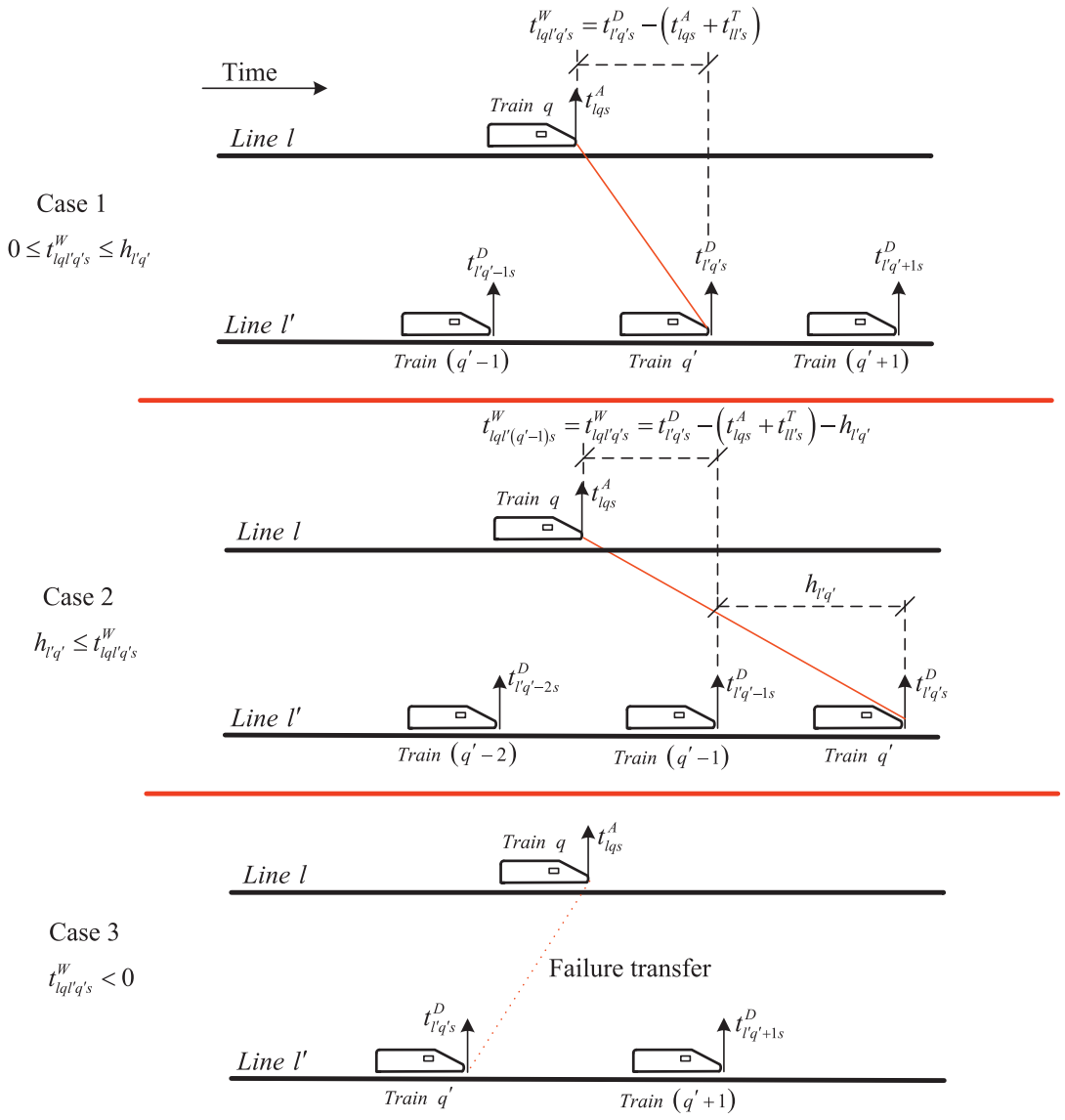


**Fig. 5.** Three cases of PWT.

and the first arriving train which can be taken on successful in line $l$'; in case 3, when passengers from the train $q$ missed the connection of train $q$' in line $l$', let $t^{W}_{lql'q's}=\infty$. This measure represents that passengers would not travel by this train for an overlong waiting time. Eq. (1) summaries the unified calculating method of PWT.

$$t^{W}_{lql'q's}=\begin{cases} t^{D}_{l'q's}-\left(t^{A}_{lqs}+t^{T}_{ll's}\right); & 0\le t^{D}_{l'q's}-\left(t^{A}_{lqs}+t^{T}_{ll's}\right)<h_{l'q'} \\ t^{D}_{l'q's}-\left(t^{A}_{lqs}+t^{T}_{ll's}\right)-H\times h_{l'q'}; & h_{l'q'}\le t^{D}_{l'q's}-\left(t^{A}_{lqs}+t^{T}_{ll's}\right) \\ \infty; & t^{D}_{l'q's}-\left(t^{A}_{lqs}+t^{T}_{ll's}\right)<0 \end{cases} \tag{1}$$

where $H=[(t^{D}_{l'q's}-(t^{A}_{lqs}+t^{T}_{ll's}))/h_{l'q'}]$, and this term denotes the train numbers running in connecting line $l$' when feeder passengers arrive at the platform before they ridding on.

Herein, let $t^{TS}_{lql'q's}$ denote the train synchronization time (TST). It could be calculated by $t^{D}_{l'q's}-(t^{A}_{lqs}+t^{T}_{ll's})$, when the passengers can transfer successfully from the train $q$ in line $l$ to train $q$' in line $l$' (case 1 and case 2). In case 1, TST is equals to PWT; however in case 2, the TST is longer than PWT. If one passenger fails to transfer, the value of $t^{TS}_{lql'q's}$ also approaches infinity.

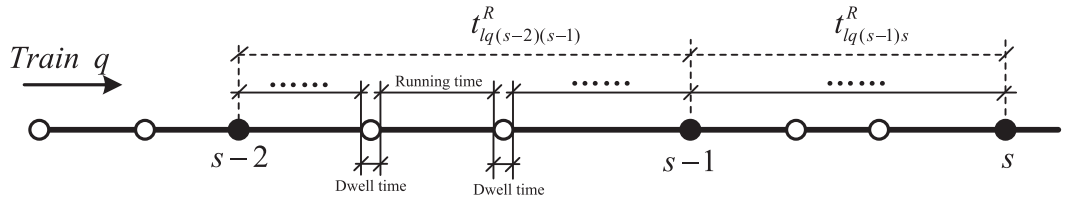


**Fig. 6.** Illustration of running time in MTN.

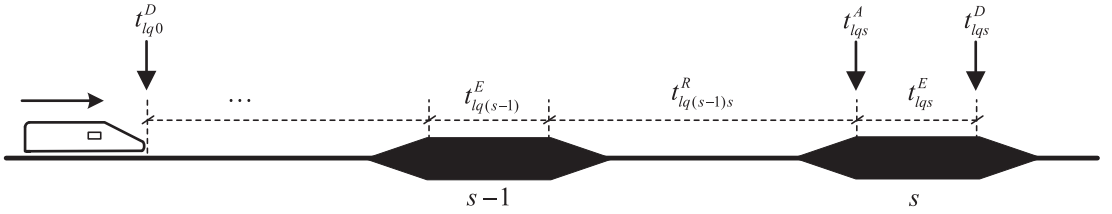


**Fig. 7.** Illustration of departure time and arrival time in MTN.

### 3.4. Formulation

#### 3.4.1. Objective function

The definition of synchronization is the separation time between two trains (belonging to different lines or different periods), which can satisfy within a specific time window at station $s$ instead of arriving at the same time in this paper. Note that the synchronization belonging to different time periods should be merged in one timetable to cover a given planning horizon. The minimum value of the transfer time window for synchronization should be larger than zero and the maximum value should no more than limits of passengers' waiting tolerance. Synchronization events depend on the departure time, running time, dwell time, and waiting time of trains. Thus, the decision variables are departure time, running time, dwell time and headway. We define an auxiliary binary variable $\theta_{lql'q's}$ to count a synchronization of train $q$ in line $l$ and train $q$' in line $l$' at station $s$:

$$\theta_{lql'q's} = \begin{cases} 1, & \text{if the train } q \text{ in line } l \text{ can synchronize with train } q' \text{ in line } l' \text{ at station } s; \\ 0, & \text{otherwise.} \end{cases}$$

In order to guarantee the smooth transitions of train services between consecutive time periods, we maximize the number of synchronizations within the planning horizon.

$$Z_{TSTP} = \max \sum_{l,l' \in L} \sum_{s \in S(l) \cap S(l')} \sum_{q=1}^{N_l} \sum_{q'=1}^{N_{l'}} \theta_{lql'q's} \tag{2}$$

#### 3.4.2. Train operation constraints

To simplify the problem, the running time and the dwell time of non-transfer stations between two transfer stations are merged as shown in Fig. 6.

For each line, constraints (3) and (4) track the arrival time $t^A_{lqs}$ and the departure time $t^D_{lqs}$ of the train $q$ in line $l$ at transfer station $s$. The detailed explanation is given in Fig. 7 where $t^D_{lq0}$ is the departure time in the origin of line $l$.

$$t^A_{lqs} = t^D_{lq0} + \sum_{s \in S(l)} t^R_{lq(s-1)s} + \sum_{s \in S(l)-1} t^E_{lqs};\ \forall l \in L, q = 1, 2 \ldots N_l \tag{3}$$

$$t^D_{lqs} = t^A_{lqs} + t^E_{lqs};\ \forall l \in L, q = 1, 2 \ldots N_l, s \in S(l) \tag{4}$$

where $\sum_{s \in S(l)} t^R_{lq(s-1)s}$ and $\sum_{s \in S(l)-1} t^E_{lqs}$ represent the running time and dwell time of the train $q$ from its original station to station $s$ in line $l$, respectively.

The limits on the dwell time and running time for the train $q$ should be satisfied to ensure operational safety, which are shown in constraints (5)–(10). $t^R_{lq(s-1)s,\min}$ and $t^R_{lq(s-1)s,\max}$ denote minimum and maximum running time of train $q$ in line $l$ from transfer station $(s-1)$ to transfer station $s$, respectively. $t^E_{lqs,\min}$ and $t^E_{lqs,\max}$ are minimum and maximum dwell time of train $q$ at transfer station $s$ in line $l$; and $\tilde{t}^R_{lq(s-1)s}$ and $\tilde{t}^E_{lqs}$ are buffer running time of train $q$ in line $l$ from transfer station $(s-1)$ to transfer station $s$. Subsequently, in line $l$, $\tilde{t}^E_{l,\max}$ and $\tilde{t}^R_{l,\max}$ are the predetermined maximal sum of buffer dwell time at all stations and buffer running time in all sections. Constraints (7) and (10) ensure that the train stopover time at each

station and section have a feasible range, with an upper bound of $\tilde{t}^{E}_{l,\max}$ and $\tilde{t}^{R}_{l,\max}$ for the total buffer time to maintain a reasonable travel.

$$t^{E}_{lqs,\min} \le t^{D}_{lqs} - t^{A}_{lqs} \le t^{E}_{lqs,\max};\ \forall l \in L, q = 1,2\ldots N_l, s \in S(l) \tag{5}$$

$$\tilde{t}^{E}_{lqs,\min} \le \tilde{t}^{E}_{lqs} \le \tilde{t}^{E}_{lqs,\max};\ \forall l \in L, q = 1,2\ldots N_l, s \in S(l) \tag{6}$$

$$\sum_{s\in S(l)} \tilde{t}^{E}_{lqs} \le \tilde{t}^{E}_{l,\max};\ \forall l \in L, q = 1,2\ldots N_l \tag{7}$$

$$t^{R}_{lq(s-1)s,\min} \le t^{R}_{lq(s-1)s} \le t^{R}_{lq(s-1)s,\max};\ \forall l \in L, q = 1,2\ldots N_l, s \in S(l) \tag{8}$$

$$\tilde{t}^{R}_{lq(s-1)s,\min} \le \tilde{t}^{R}_{lq(s-1)s} \le \tilde{t}^{R}_{lq(s-1)s,\max};\ \forall l \in L, q = 1,2\ldots N_l, s \in S(l) \tag{9}$$

$$\sum_{s\in S(l)} \tilde{t}^{R}_{lq(s-1)s} \le \tilde{t}^{R}_{l,\max};\ \forall l \in L, q = 1,2\ldots N_l \tag{10}$$

Constraint (11) is used to ensure that the departure time of first trains at any stations would not be earlier than $A$ and not later than $B$, where $A$ and $B$ are constants published by companies. At station $s$ of line $l$, the departure time first train is denoted by $t^{D}_{l1s}$, the dwell time at station $s$ is denoted by $t^{E}_{l1s}$, and $t^{D}_{l10}$ is the departure time of first train in the origin of line $l$.

The running time between station $(s-1)$ and station $s$ of first train in line $l$ is denoted by $t^{R}_{l1(s-1)s}$.

$$A \le t^{D}_{l10} + \sum_{s\in S(l)} t^{R}_{l1(s-1)s} + \sum_{s\in S(l)} t^{E}_{l1s} \le B;\ \forall l \in L \tag{11}$$

### 3.4.3. Safety headway constraints

Operational requirements on headways for different trains should be satisfied to ensure operating safety. If the transitional period satisfied the peak period to off-peak period, the headway of latter trains should be longer to avoid the mutation of headway in various time period, denoted as $h_{l(q-1)} \le h_{lq}$. Otherwise, $h_{l(q-1)} \ge h_{lq}$. The headway of two consecutive trains should satisfy constraint (12). Constraint (13) ensures the upper and lower bounds of headways.

$$h_{lq} + t^{D}_{lqs} = t^{D}_{l(q+1)s};\ \forall l \in L, q = 1,2\ldots N_l, s \in S(l) \tag{12}$$

$$h_{lq,\min} \le h_{lq} \le h_{lq,\max};\ \forall l \in L, q = 1,2\ldots N_l \tag{13}$$

### 3.4.4. Transfer efficiency constraints

The ratio of the number of passengers (boarding train $q$ successfully and heading toward train $q$') to the total passengers in the planning period $[T_1, T_2]$ is denoted by the transfer efficiency $\partial$. Constraint (14) ensures that the stations with more transfer passengers have priority and passenger attendances should also be ensured by companies pursuing their own benefit. Subsequently, this constraint is nonlinear and the time indexes are applied to distinguish different periods, i.e., the peak period, the transitional period and the off-peak period.

$$\frac{\sum_{t\in[T_1,T_2]}\sum_{l,l'\in L}\sum_{s\in S(l)\cap S(l')}\sum_{q=1}^{N_l}\sum_{q'=1}^{N_{l'}}\left(\theta_{lql'q's}\times P^{H,t}_{lql'q's}\right)}{\sum_{t\in[T_1,T_2]}\sum_{l,l'\in L}\sum_{s\in S(l)\cap S(l')}\sum_{q=1}^{N_l}\sum_{q'=1}^{N_{l'}} P^{H,t}_{lql'q's}} \ge \partial \tag{14}$$

### 3.4.5. TST constraints

Constraints (15)–(19) describe the passengers' transfer status (successful or failure) among different trains in MTN. Constraints (15) and (16) allow the synchronization variables $\theta_{lql'q's}$ be activated if the difference between arrivals of train $q$ in line $l$ and train $q$' in line $l$' at station $s$ is between a separation time window $[t^{W}_{lql'q's}, T_a]$. $T_a$ is the maximum acceptable connection times of passengers. Moreover, in Constraint (17), another binary variable $D_{lql'q's}$ which has the same domain with $\theta_{lql'q's}$ is given to illustrate successful synchronization. $M$ is an arbitrarily large number. If the model is calculated by the formula $t^{TS}_{lql'q's} \ge t^{W}_{lql'q's} - M\times(1-\theta_{lql'q's})$ directly, this term $M\times(1-\theta_{lql'q's})$ can be divided into $M - M\times\theta_{lql'q's}$, which means $\theta_{lql'q's}$ is an invalid variable in this constraint. Finally, constraints (18) and (19) represent the domain of the decision variables.

$$t^{TS}_{lql'q's} \ge t^{W}_{lql'q's} - M\times D_{lql'q's};\ \forall l \in L, l' \in L, q = 1,2\ldots N_l, q' = 1,2\ldots N_{l'}, s \in S(l)\cap S(l') \tag{15}$$

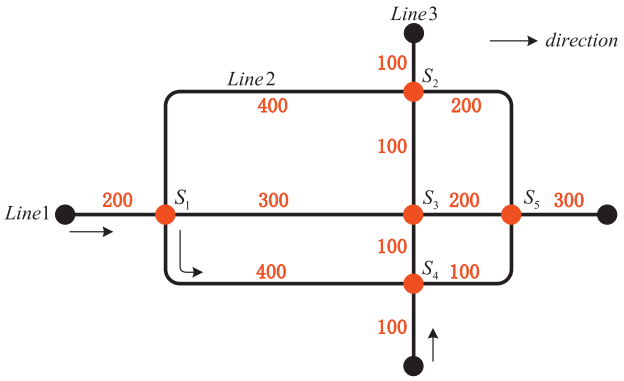


**Fig. 8.** Illustration of the sample network.

$$t^{TS}_{lql'q's} \le T_a + M \times D_{lql'q's}; \forall l \in L; q = 1, 2 \ldots N_l; q' = 1, 2 \ldots N_{l'}; s \in S(l) \cap S(l') \tag{16}$$

$$\theta_{lql'q's} = 1 - D_{lql'q's}; \forall l \in L, l' \in L, q = 1, 2 \ldots N_l, q' = 1, 2 \ldots N_{l'}, s \in S(l) \cap S(l') \tag{17}$$

$$\theta_{lql'q's} \in \{0, 1\}; \forall l \in L, l' \in L, q = 1, 2 \ldots N_l, q' = 1, 2 \ldots N_{l'}, s \in S(l) \cap S(l') \tag{18}$$

$$D_{lql'q's} \in \{0, 1\}; \forall l \in L, l' \in L, q = 1, 2 \ldots N_l, q' = 1, 2 \ldots N_{l'}, s \in S(l) \cap S(l') \tag{19}$$

*3.4.6. Formulation complexity*

The computational complexity theory focuses on classifying problems according to their inherent difficulty, and relating those classes to each other. There are a number of difficulties in solving the timetabling problem, and we analyze the complexity of the proposed mixed integer nonlinear programming model. We prove that the train synchronization timetabling problem belongs to the NP-hardness class which can be reduced by an NP-Complete problem. The detailed proof can be found in Appendix A.

## 4. Solution algorithm and numerical experiment

The branch-and-bound method is a feasible method to find optimal solutions in solving mixed integer nonlinear programming which is proposed in this paper. However, it cannot guarantee short computation time as that depends on the degree of successful pruning which itself depends on the problem definition. Additionally, due to the NP-hardness complexity of the train synchronization timetabling problem which has been proved in Appendix A, i.e., the branch-and-bound method is adopted only in the simple example in Section 4.2. Numerical examples show that heuristic algorithms have many advantages, such as small calculation quantity, high accuracy and wide application in real-world cases. Thus, to solve this optimization problem, a heuristic approach based on PSO and SA algorithm is explained in Section 4.1. A numerical example is discussed in Section 4.2 and 4.3. The branch-and-bound method, GA, SA, PSO and hybrid PSO-SA algorithms are compared in Section 4.3.

### *4.1. Particle swarm optimization and simulated annealing algorithm*

PSO-SA takes the advantage of superior convergence performance of PSO and local search capability of SA (Niknam et al., 2009; Idoumghar et al., 2011; Zhu, 2009). It produces solutions in a reasonable time that is good enough for solving NP-hardness problem. Key steps of the PSO-SA algorithm are explained as follows:

(1) Solution encoding. Each particle $X$ is represented by its components, in this problem, the variables are the departure time of first trains, the running time, dwell time and the headways among trains in all lines, which are all integer, denoted by $X = \{t^D_{111} \ldots t^D_{m11}, t^E_{111} \ldots t^E_{m1n}, t^R_{1112} \ldots t^R_{m1(n-1)n}, h_{11} \ldots h_{mN_l}\}$, where $m$ represents the number of lines, $n$ represents the total number of the stations and $N_l$ represents the numbers of trains in line $l$. $(m+n\times m+(n-1)\times m+(N_l-1)\times m)$ represents the dimension of the problem to solve. Fig. 8 is a sample network containing three lines and five transfer stations. The arrow on each line indicates the direction. The original running time between two consecutive stations are marked with red number, and the transfer walking time is assumed to be 0.5 minutes. A sample encoding of the network, which is first divided into four sections for the first departure time, dwell time and running time, is shown in Fig. 9. The value represents the first departure time of lines, station dwell

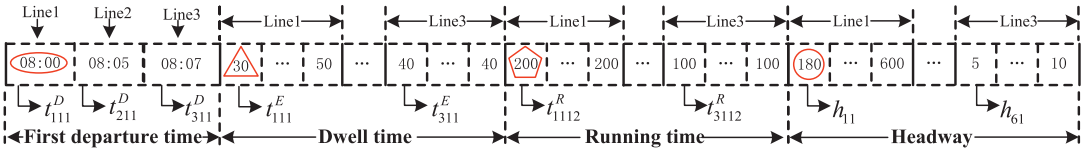


**Fig. 9.** Encoding for the sample network.

time, interval running time and headway in each cell of the subsection. For instance, the oval part in Fig. 9 represents the first train's departure time of the up direction of line 1, or 08:00. The triangle value indicates that the first train will stop at station $S_1$ for 30 s. Meanwhile, the quinquangular part indicates that the first train in this line takes 200 s to run to station $S_1$ and the circled part indicates that the second train in up direction of line 1 will depart 180 s later behind the first train.

(2) Initialization. Initial swarm corresponds to population of particles. Each particle is initialized with the uniform random value (position and velocity) between the lower and upper boundaries of the interval defining in the objective function.

(3) The fitness function of a solution is evaluated by the objective function (2).

(4) Update. Updating the position and velocity according to the following rules, where $c_1$ and $c_2$ are two learning factors which control the influence of the social and cognitive components (usually,$c_1 = c_2 = 2$, see Idoumghar et al., 2011; Shi and Eberhart, 1999); $r_1$ and $r_1$ are distributed random numbers within the range of [0, 1]. At each generation, the particles are updated by using following two best values. The first value is the best fitness a particle has achieved so far. This value is called $p_b$. The second value is the best value tracked by the particle swarm optimizer so far in the population. This best value is a global best solution and is called $p_g$.

$$v(i+1) = \varphi\{v(i) + c_1 r_1[p_b(i) - x(i)] + c_2 r_2[p_g(i) - x(i)]\}$$
$$x(i+1) = x(i) + v(i+1)$$

where $\varphi = \frac{2}{|2-C-\sqrt{C^2-4C}|}, C = c_1 + c_2$.

(5) SA algorithm. The performance of SA depends on the definition of the several control parameters. (a) Initial Temperature. $\dot{T}_0$ is then given by $\dot{T}_0 = f(p_g)/\ln 5$. (b) Decrementing the temperature. The calculation of this probability relies on a parameter $\dot{T}$, which is referred to as temperature, since it plays a similar role as the temperature in the physical annealing process. To avoid getting trapped in a local minimum point, the rate of reduction should be slow. In our problem we use the following method to reduce the temperature: $\lambda = 0.9$ and $\dot{T}_{i+1} = \lambda \times \dot{T}_i$.

(6) Termination criterion. The stopping criterion defines when the system has reached the predetermined maximum number of iterations or predetermined precision $a_c$.

*The hybrid PSO-SA algorithm in this paper can be described as follows:*

Step 1: Set the initial parameters: initial population and initial velocity.
Step 2: Calculate the value of objective function for each individual.
Step 3: Sort the initial population based on the objective function values. The initial population is ascending, based on the value of the objective function.
Step 4: Select the best global position. The individual that has the minimum/maximum objective function is selected as the best global position and fitness value $p_g$.
Step 5: Apply SA to search around the global solution $p_g$. Updating $p_g$, if the solution obtained by SA is better than it.
Step 6: Select the best local position for each individual.
Step 7: Select the *i*th individual and update the position and velocity. The modified position for the *ith* individual is checked with its boundary.
Step 8: Decrease the temperature.
Step 9: Check the termination criteria. If they are satisfied with the termination criteria, the algorithm terminates; otherwise, then go back to Step 3. The flowchart of PSO-SA is shown in Fig. 10.

### 4.2. Numerical example

To prove the efficiency of PSO-SA, a numerical example serves as a case to illustrate the proposed model. The references dwell time and headways in the peak/off-peak period at transfer stations are given in Table 3 (See Fig. 8). Both adjustment range of the running time and dwell time between two consecutive stations are given as [−5, 5].

The experiments are tested on a personal computer with an Intel core i3, 2.13 GHz CPU and 8GB RAM. We consider the problem under the second-dependent and the optimal departure time of the first train in each line are given in Table 4.

This model and the following constraints are adopted to avoid the mutation of headway in various time periods, which will short the passengers' travel time (see Fig. 11). The vertical axis and horizontal axis in Fig. 11 stand for travel time and entry time for passenger respectively.

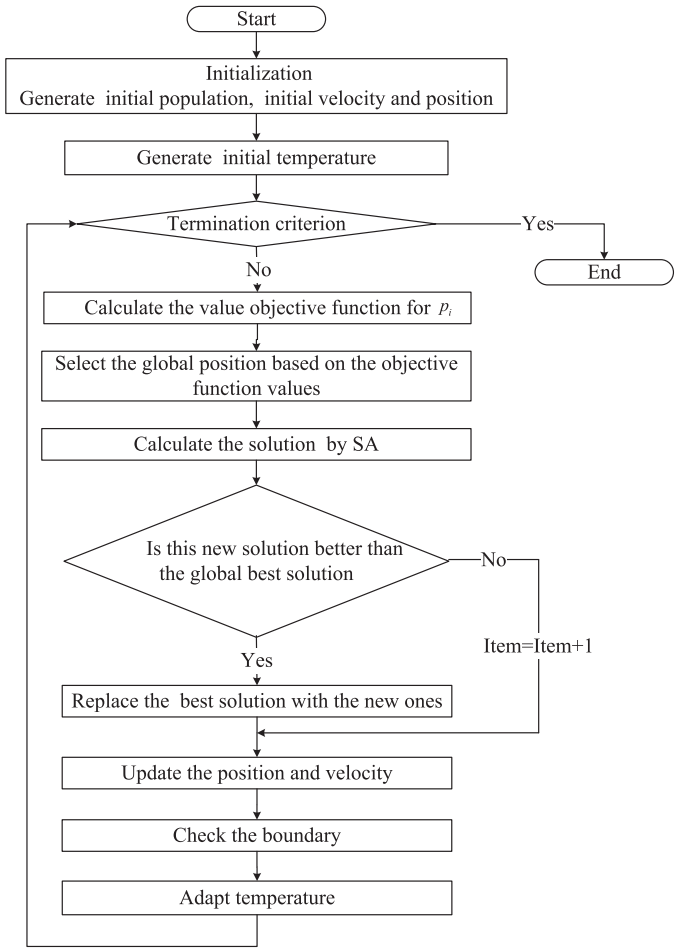


**Fig. 10.** The flowchart of PSO-SA.

**Table 3**
The reference headway and reference dwell time at all transfer stations (second).

| **Station** | $S_1$ | $S_2$ | $S_3$ | $S_4$ | $S_5$ | Headway (s) | |
|---|---|---|---|---|---|---|---|
| | | | | | | Peak period | Off-peak period |
| **Line 1** | 30 | – | 30 | – | 50 | 180 | 600 |
| **Line 2** | 40 | 50 | – | 50 | 40 | 180 | 600 |
| **Line 3** | – | 40 | 30 | 40 | – | 180 | 600 |

### *4.3. Algorithm comparison*

In this section, the results of PSO-SA are compared with other methods, such as the branch-and-bound, GA, SA and PSO methods. Calculation results are given in Table 5, which demonstrates that all solution algorithms could obtain similar results and the heuristic algorithms have a higher efficiency. Therefore, the PSO-SA is used to solve the large scale problem of Beijing metro network. The following conclusions are put forward here.

(1) Similar optimized results (in terms of objective function values) are obtained except for SA. The branch-and-bound method, PSO-SA, GA and PSO can improve the objective function from 92 to 215, in comparison with the original value.
(2) Heuristic algorithms compute more quickly than the branch-and-bound method. It takes an average of 92.56 s to obtain an optimal solution for heuristic algorithms. However, the branch-and-bound method takes 3077.03 s, which would imply low efficiency and practicality.
(3) Computational efficiency varies among heuristic algorithms. PSO-SA, GA and PSO take 79.33 s, 128.04 s, and 87.84 s respectively (SA has trapped in local optimal solution). Clearly, PSO-SA is very effective in CPU time.

**Table 4**
Optimal departure time and headway for the test network.

| Line | Transfer station (s) | | | | | | Headway (s) | | | |
|---|---|---|---|---|---|---|---|---|---|---|
| | $S_1$ | $S_2$ | $S_3$ | $S_4$ | $S_5$ | Peak period | Transitional period | | | Off-peak period |
| | | | | | | | Train 1 | Train 2 | Train 3 | |
| **Line 1** | 225 | – | 555 | – | 798 | 180 | 186 | 205 | 181 | 600 |
| **Line 2** | 16 | 833 | – | 455 | 597 | 180 | 320 | 328 | 327 | 600 |
| **Line 3** | – | 491 | 356 | 230 | – | 180 | 462 | 468 | 468 | 600 |

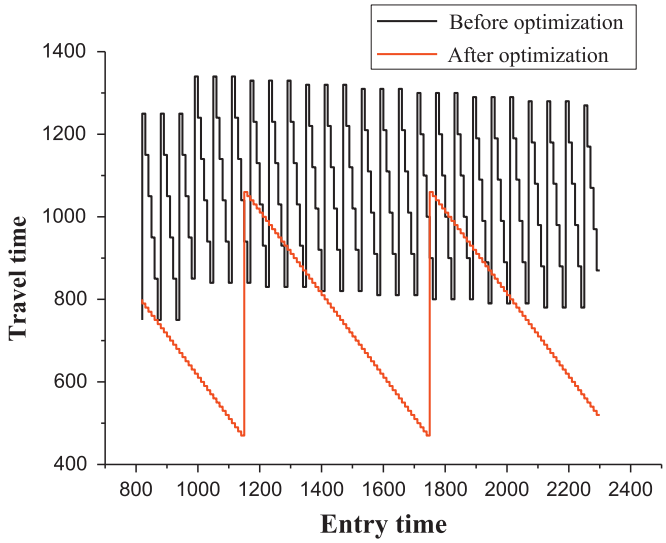


**Fig. 11.** Travel time in the sample test.

**Table 5**
Results of model solved by different algorithms.

| Method | CPU (s) | Objective | Improvement (%) |
|---|---|---|---|
| Original | – | 92 | – |
| Branch-and-bound | 3077.03 | 215 | 156.52 |
| SA | 75.00 | 214 | 132.60 |
| PSO | 87.84 | 215 | 156.52 |
| GA | 128.04 | 215 | 156.52 |
| PSO-SA | 79.33 | 215 | 156.52 |

## 5. Case study

In this section we apply the proposed modeling framework to the Beijing metro network. Section 5.1 presents the main features of this network. Section 5.2 reports the optimal results and the evaluation indicators.

### 5.1. Beijing metro network

(1) The Beijing metro network has 42 transfer stations and 16 lines (bi-directional) in all. As seen from Fig. 12, the direction of a solid arrow on a line represents up-train direction, and the opposite direction of the same line indicates the down-train direction.
(2) To design a more realistic timetable, the directions need to be picked out for different types at transfer stations from the network. Currently, there are eight transfer directions at Crisscross transfer station (e.g., DongDan station in the Beijing metro network, see Fig. 13) and sixteen transfer directions at Triple-1ine transfer station (e.g., XiZhiMen station in the Beijing metro network, see Fig. 14), while T cross creates four directions (e.g., National library station in the Beijing metro network, see Fig. 15) and connection point has two directions (e.g., SiHui station in the Beijing metro network, see Fig. 16).
(3) Parameters in PSO-SA
(Table 6)

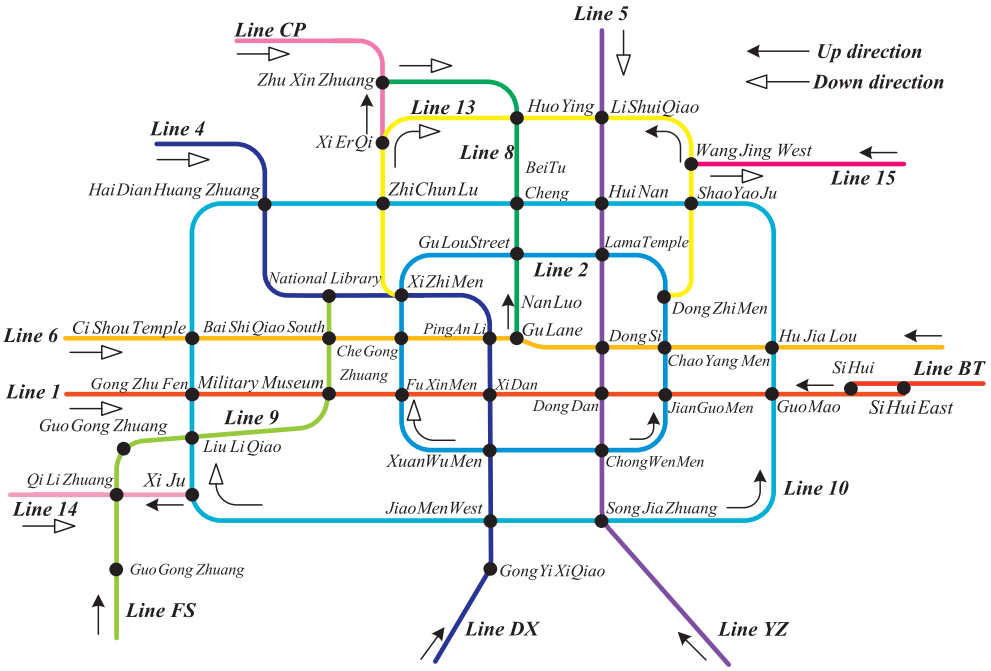


**Fig. 12.** Beijing metro network.

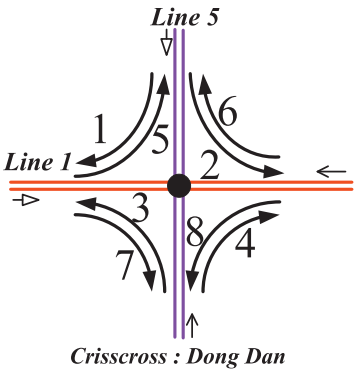


**Fig. 13.** Transfer directions' diagram in Crisscross transfer station.

**Table 6**
Parameters of Beijing metro network.

| Parameter | $N$ | Iteration | $\lambda$ | $C_1$ | $C_2$ | $T_a$ |
|---|---|---|---|---|---|---|
| Value | 40 | 100 | 0.9 | 2 | 2 | 1200 |
| Parameter | Number of variable | Number of trains | $\tilde{t}^R_{lqs(s-1),\max}$ | $\tilde{t}^R_{lqs(s-1),\min}$ | $\tilde{t}^E_{lqs,\max}$ | $\tilde{t}^E_{lqs,\min}$ |
| Value | 1415 | 640 | 5 | -5 | 5 | -5 |
| Parameter | Number of lines | Number of transfer stations | $a_c$ | $\partial$ | $\tilde{t}^R_{l,\max}$ | $\tilde{t}^E_{l,\max}$ |
| Value | 32 | 42 | 1.e-14 | 0.6 | 500 | 500 |

## 5.2. Results and analysis

To verify the effectiveness of the proposed model, four indicators (headway, the equilibrium coefficient, the transfer efficiency and travel time) are tested to compare the results before and after optimization during the transitional period.

(1) Headway

As mentioned above, it will increase the travel time for passengers who travel through several planning periods. One of the main causes is a great difference in the frequency on each line, for instance, the higher frequency in the peak period and the lower frequency in the off-peak period. In the transitional period, a smooth transition of frequency (headway) rather than mutation of headway becomes particularly important. In Fig. 17, the proposed method avoids the mutation of

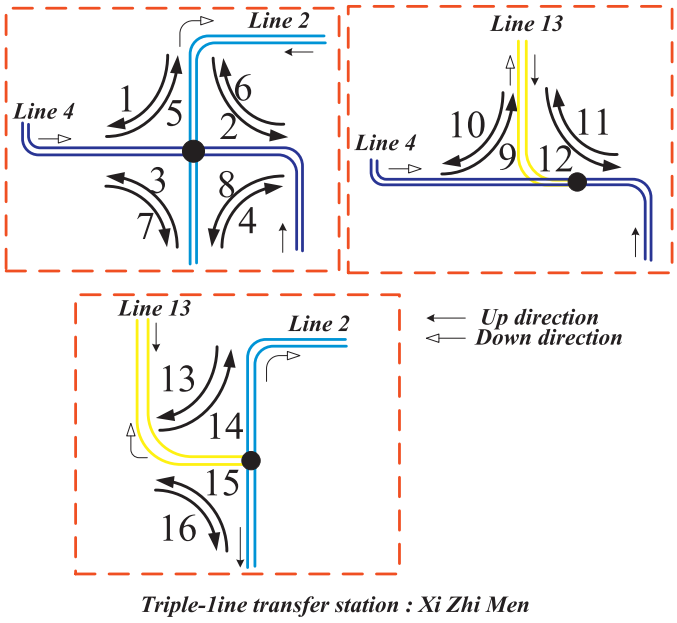


**Fig. 14.** Transfer directions' diagram in Triple-1ine transfer station.

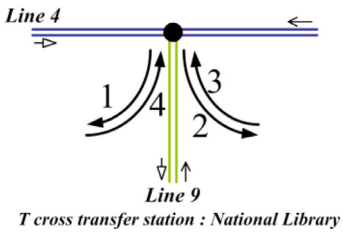


**Fig. 15.** Transfer directions' diagram in T cross transfer station.

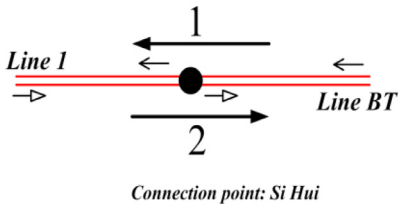


**Fig. 16.** Transfer directions' diagram in Connection point.

headways successfully in all lines of the Beijing metro network. The tendency of headway which marked by a dotted line with a red arrow (see Fig. 17) is in line with the real-world operations in the transitional period (the off-peak period to the peak period).

(2) The equilibrium coefficient

The equilibrium coefficient could represent the discrete degree of vehicle flow and robustness of the timetable network easily and directly. In a planning period, the inequitable timetable can lead to the inhomogeneity of waiting time in transfer stations, i.e. it will increase the probability of unacceptable amount for passengers' waiting time. Moreover, the discrete degree of departure time for coordination is lower, i.e., more equilibrium, the ability of tolerating perturbations is stronger for a timetable network. In Beijing metro network, this indicator represents not only the equilibrium of the timetable network, but also the discrete degree of departure time for coordination at transfer stations. The equilibrium coefficient can be calculated as follows (see Hao and Zhang, 2000):

$$EI = \left[1 - \frac{2}{(n-1)}\right]\frac{D(H_{lq})}{3} = \left[1 - \frac{2}{(n-1)}\right]\frac{E(H_{lq}^2) - E(H_{lq})^2}{3}, \forall q \in [T_1, T_2]$$

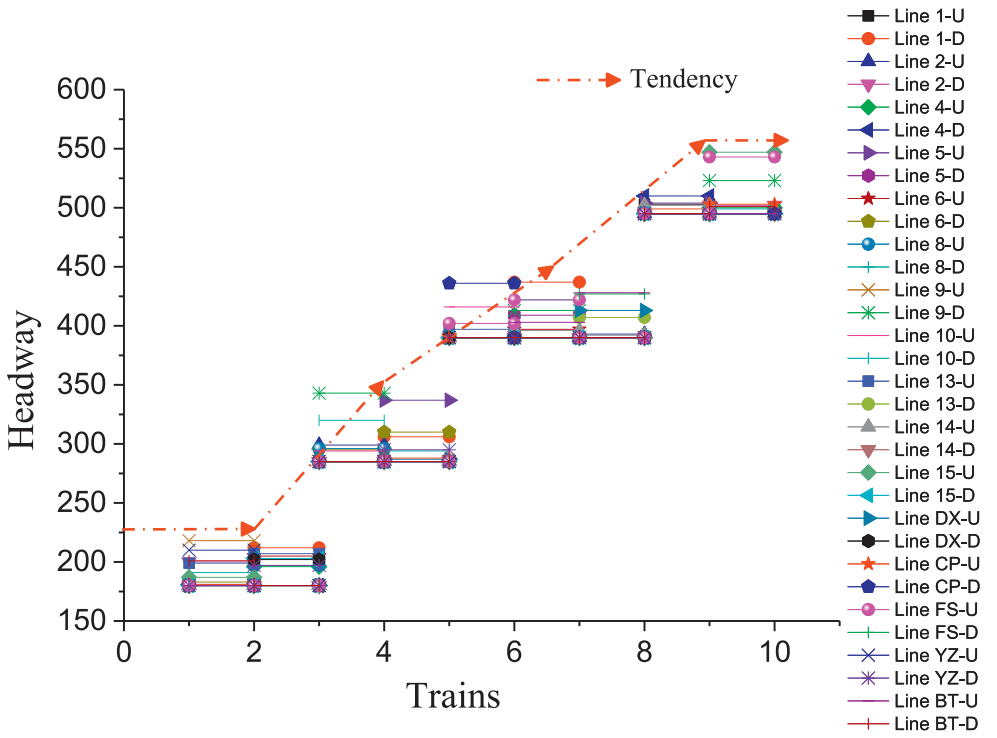


**Fig. 17.** Headways in Beijing metro network.

where $n$ is the number of headways in the time period $[T_1, T_2]$. Obviously, the smaller $EI$, the more balance of the timetable network. The equilibrium coefficient of original timetable is about 3.93, while it is about 1.14 for the optimized timetable. It is clear that the optimized timetable has a better equilibrium compared with the original one.

Besides, the train working diagram is other means to visualize the distribution of vehicle flow, which is plotted by departure/arrival time on the horizontal axis and stations of line 1 on the vertical as showed in Fig. 18. In the figure, the red line indicates the train working diagram after optimized by the suggested model in the Beijing metro network, the black line represents the original train working diagram, and the green line shows an overlap of the original and current train working diagram. We can see that the distribution of red lines is much more balanced compared with black lines.

(3) The transfer efficiency

The constraint of the transfer efficiency is an operative to balance the interests of passengers and operators. The higher value of the transfer efficiency indicates that an operator would impose restrictions on attendances in trains to increase revenue. Otherwise, the lower value can relax these restrictions may be beneficial to passengers' travel time. Table 7 shows that the larger value of transfer efficiency will help fitness function but go against revenue of operators, and synchronization numbers for the different types of transfer stations in Beijing metro network.

(4) Travel time

The smooth transition can make a contribution in decrease the travel time. Our proposed model is committed to tackling this problem with smooth transition in the transitional period. This control strategy pone to variable headways and maximize the transfer synchronization events. Thus, to appraise the distribution of vehicle flow, the equilibrium and robustness of the network, we made a comparison between the optimal timetable and the current timetable in Beijing metro. To illustrate the advantages of this model, some OD pairs are selected to verify the travel time.

(a) Only one effective shortest-route in an OD pair

Based on the real AFC (Automatic Fare Collection System) data within 08:00:00–10:00:00 in Beijing metro network, we choose an OD pair from HuiNan to XiDan as an example. With the automatic fare collection data, we can get the entry time and deal time created by records. Utilizing the lag to obtain the travel time is the truest reflection from travelers. In Fig. 19, the routes (1), (2) and (3) are all feasible on account of that all these routes can travel from origin to destination. However, the routes (2) and (3) have much longer running time and transfer time than route (1). Then, the route (1) can be regarded as the only one effective route in the real travel.

Table 8 illustrates the improvement of travel time in comparison with the real AFC data. The average walking time for entry HuiNan station is 51 s and get off of the XiDan station is 40 s, which are all obtained from the field survey.

(b) Several effective routes in an OD pair

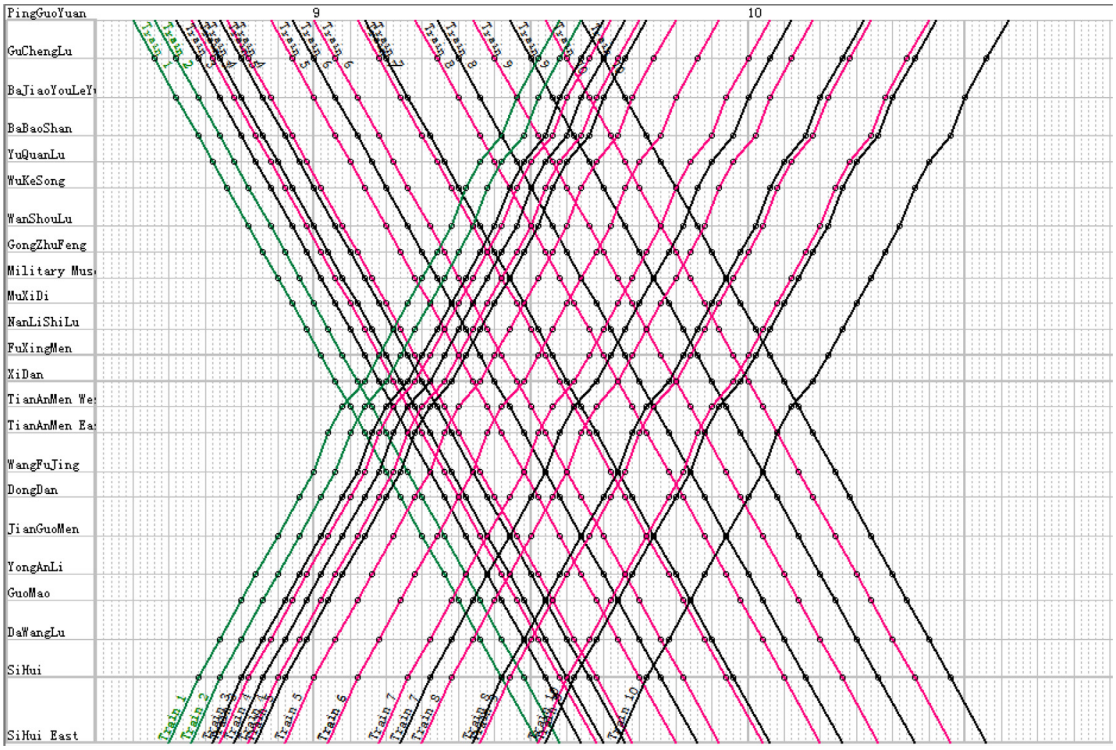


**Fig. 18.** Train working diagram of line 1 in Beijing metro network.

**Table 7**
Parameters for different transfer efficiency.

| | Items | transfer efficiency $\partial$ | | | | | |
|---|---|---|---|---|---|---|---|
| | | | 0.3 | 0.4 | 0.5 | 0.6 | 0.7 |
| | **Iterations** | | 100 | 100 | 100 | 100 | 100 |
| | **Iterations in convergence point** | | 6 | 64 | 30 | 45 | 65 |
| | **Number of trains** | | 20 | 20 | 20 | 20 | 20 |
| | **Objective** | | 7399 | 7306 | 7293 | 7273 | 7246 |
| **Crisscross** | **Number of transfer stations** | | | | 30 | | |
| | **Number of transfer directions** | | | | 8 | | |
| | **Synchronization numbers** | **Sum** | 5674 | 5570 | 5590 | 5560 | 5510 |
| | | **Average** | 24 | 23 | 23 | 23 | 23 |
| **Triple-1ine** | **Number of transfer stations** | | | | 2 | | |
| | **Number of transfer directions** | | | | 16 | | |
| | **Synchronization numbers** | **Sum** | 792 | 792 | 791 | 784 | 795 |
| | | **Average** | 25 | 25 | 25 | 25 | 25 |
| **T cross** | **Number of transfer stations** | | | | 7 | | |
| | **Number of transfer directions** | | | | 4 | | |
| | **Synchronization numbers** | **Sum** | 770 | 778 | 753 | 767 | 780 |
| | | **Average** | 27 | 28 | 27 | 27 | 28 |
| **Connection point** | **Number of transfer stations** | | | | 3 | | |
| | **Number of transfer directions** | | | | 2 | | |
| | **Synchronization numbers** | **Sum** | 163 | 166 | 159 | 162 | 161 |
| | | **Average** | 27 | 28 | 27 | 27 | 27 |

Based on the real AFC data, the real travel time can be extracted from GongZhuFen to ChongWenMen by the trip card (see Fig. 20). In this case, one route is chosen randomly from two effective routes to show the improvement of travel time by the proposed method (see Table 9). The average walking time for entry GongZhuFen station is 51 s and get off of the ChongWenMen station is 110 s, which are all obtained from the field survey.

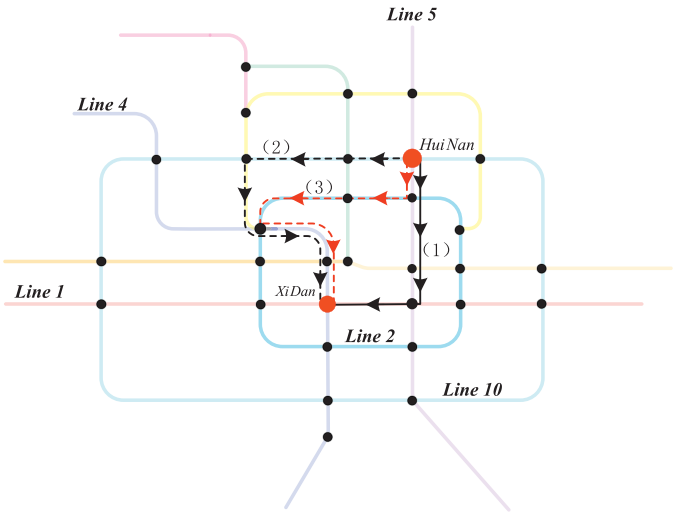


**Fig. 19.** Three travel routes from HuiNan to XiDan.

**Table 8**
Travel time comparison from HuiNan to XiDan.

| Origin-destination | | Real AFC data | | Optimized timetable | | | |
|---|---|---|---|---|---|---|---|
| | Entry time | Deal time | Travel time | Aboding time | Arrival time | Travel time | Improvement (%) |
| **HuiNan–XiDan** | 9:04:00 | 9:38:07 | 0:34:07 | 9:07:19 | 9:34:25 | 0:31:05 | 8.89 |
| | 9:07:00 | 9:38:14 | 0:31:14 | 9:10:19 | 9:34:25 | 0:28:05 | 10.09 |
| | 9:09:00 | 9:42:23 | 0:33:23 | 9:14:19 | 9:40:55 | 0:32:35 | 2.40 |
| | 9:10:00 | 9:45:27 | 0:35:27 | 9:14:19 | 9:40:55 | 0:31:35 | 10.91 |
| | 9:16:00 | 9:52:01 | 0:36:01 | 9:19:49 | 9:49:18 | 0:33:58 | 5.69 |
| | 9:17:00 | 9:50:10 | 0:33:10 | 9:19:49 | 9:49:18 | 0:32:58 | 0.60 |

Note: The time is represented in the 24-h HH:MM:SS format.

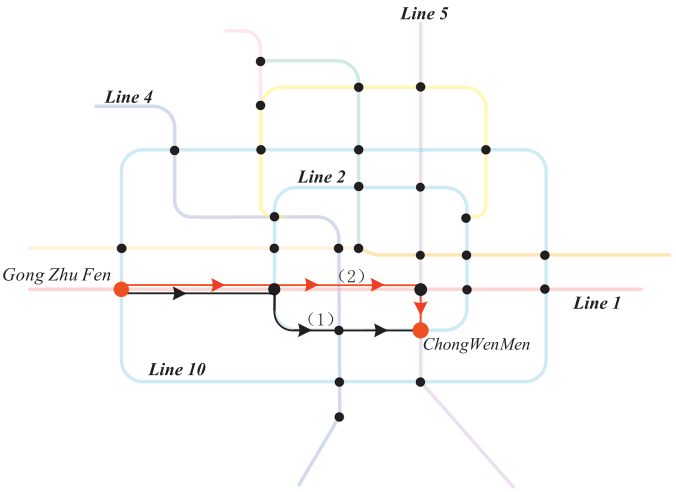


**Fig. 20.** The routes of GongZhuFen to ChongWenMen.

## 6. Conclusion

Considering of the significant travel demand change during the transitional period from peak to off-peak hours or vice versa, this study tackles the transitional period train timetable optimization problem for MTN. A mixed integer nonlinear programming model is developed to adjust the train timetables according to time-varying travel demand and maximize the transfer synchronization in MTN. An effective PSO-SA solution method is proposed to obtain solutions for real-world large-scale networks. Additionally, detailed analysis on key parameters is conducted to demonstrate the effectiveness of the

**Table 9**
Travel time comparison from GongZhuFen to ChongWenMen.

| Origin-destination | | Real AFC data | | Optimized timetable | | | Improvement (%) |
|---|---|---|---|---|---|---|---|
| | Entry time | Deal time | Travel time | Departure time | Arrival time | Travel time | |
| **GongZhuFen–ChongWenMen** | 9:06:00 | 9:41:24 | 0:35:24 | 9:10:40 | 9:34:15 | 0:28:15 | 20.20 |
| | 9:09:00 | 9:37:14 | 0:28:14 | 9:10:40 | 9:34:15 | 0:25:15 | 10.57 |
| | 9:14:00 | 9:44:09 | 0:30:09 | 9:15:25 | 9:39:00 | 0:25:00 | 17.08 |
| | 9:27:00 | 9:58:02 | 0:31:02 | 9:28:25 | 9:52:00 | 0:25:00 | 19.44 |
| | 9:32:00 | 10:02:06 | 0:30:06 | 9:34:55 | 9:58:30 | 0:26:30 | 11.96 |
| | 9:33:00 | 10:04:10 | 0:31:10 | 9:34:55 | 9:58:30 | 0:25:30 | 18.18 |
| | 9:40:00 | 10:10:12 | 0:30:12 | 9:43:18 | 10:06:53 | 0:26:53 | 10.98 |

Note: The time is represented in the 24-h HH:MM:SS format.

developed model. The Beijing metro network case shows that the coordinated timetable is more balanced in that the smooth transition significantly reduces the passenger travel time.

There are several future research directions for the metro timetable optimization problem studied in this paper. Firstly, weights for lines, transfer stations or transfer directions will be assigned for each simultaneous arrival train to divide the transitional period exactly. For example, passenger always transfer from residence to work place in the morning. Thus, this type of the transitional period will be different with types of the transitional period in the afternoon. Secondly, the variable stop patterns can be considered to synchronize more trains in the transitional period. In addition, exact methods can be explored to improve solution quality in the large search space. Finally, in actual operations trains may miss their schedules, so it is worth discussing whether the train should wait for the delayed feeder trains.

## Acknowledgments

Dr. Sun was supported by the National Natural Science Foundation of China (71322102, 71621001). Dr. Wu was supported by the NSFC (71525002) and the Fundamental Research Funds for the Central Universities (2016JBZ007). X. Guo was supported by the China Scholarship Council. J. Zhou was supported by the National Natural Science Foundation of China (61672002). Dr. Jin was supported by the National Natural Science Foundation of China (71401101). In addition, we would appreciate the editor and reviewers for their helpful comments and suggestions, which greatly improved this paper.

## Appendix A. Computational complexity proof

To prove the train synchronization timetabling problem belongs to the NP-hardness class, the general approach is to find a proved NPC (NP-Complete) problem, which is reducible to the train synchronization timetabling problem. Reduction, especially in the NP-hardness, is a common method of proof and it is given the symbol $<=$, for example, $P <= Q$, i.e., $P$ is reducible to $Q$. More precisely, the problem $Q$ is NP-hardness when every problem $P$ in NP can be reduced in polynomial time. As it can be seen in Ibarra-Rojas and Rios-Solis (2012), NAE-3SAT belongs to NP-completeness which can be used as a starting point for proving the problem is NP-hardness.

| | |
|---|---|
| Problem *P*: NAE-3SAT | |
| INPUT | A set of Boolean variable with finite limit $X = \{x_1, x_2 \dots x_n\}, \lvert X\rvert = \tilde{n}$, and a set of clauses $C = \{C_1, C_2 \dots C_m\}, \lvert C\rvert = \tilde{m}$. Each clause $C_i$ is a formula in conjunctive normal form which has three variables, i.e., $z_1 \vee z_2 \vee z_3$. |
| Question | For a Boolean variable set $X$ and a clauses set $C$, if there exists a assignment of true values whose $\sigma = C_1 \wedge C_2 \wedge C_3$ is true? |
| Example | $X=\{x_1, x_2, x_3\}, C=\{C_1, C_2, C_3\}, \sigma = (x_1 \vee \bar{x}_2) \wedge (\bar{x}_1 \vee x_2 \vee x_3) \wedge \bar{x}_1$. Choosing $x_1 = FALSE$, $x_2 = FALSE$, and $x_3$ arbitrarily, since $\sigma = (FALSE \vee TRUE) \wedge (TRUE \vee FALSE \vee x_3) \wedge TRUE$, and in turn to $\sigma = TRUE \wedge TRUE \wedge TRUE$ (i.e. to TRUE). |
| Problem *Q*: Train synchronization timetabling problem | |
| INPUT | Parameters $L$, $S(l)$, $A$, $B$, $[T_1, T_2]$, $T_a$, $t^R_{lqs(s-1),\min}$, $t^R_{lqs(s-1),\max}$, $\tilde{t}^R_{lqs(s-1)}$, $t^E_{lqs,\min}$, $t^E_{lqs,\max}$, $\tilde{t}^E_{lqs}$, $t^T_{ll's}$, $h^p_{l,\min}$, $h^p_{l,\max}$, $P^H_{lql'q's}(t)$; $\forall l \in L$, $\forall s \in S(l)$, $t \in [T_1, T_2]$ and a scalar $K > 0$. |
| Question | Question If there exists groups of solutions on $t^A_{lqs}$, $t^D_{lqs}$, $t^R_{lqs(s-1)}$, $t^E_{ls}$, $h_{lq}$, $\theta_{lql'q's}$, $\forall l \in L$, $l' \in L$, $q=1, 2 \dots N_l$, $q'=1, 2 \dots N_{l'}$, $s \in S(l) \cap S(l')$ that satisfy constraints (3)-(19) and $\sum_{l,l' \in L} \sum_{s \in S(l) \cap S(l')} \sum_{q=1}^{N_l} \sum_{q'=1}^{N_{l'}} \theta_{lql'q's} \geq K$? |

The basic two processes which are as follow to prove that decision version of the train synchronization timetabling problem is in NP-complete.

(1) The first step is to proof this problem is in NP.

There is no known way to find an answer in polynomial time, i.e., that's the time to complete the task varies as a polynomial function on the size of the input to the algorithm, but if one is provided with information showing what the answer is, it is possible to verify the answer quickly. The class of questions for which an answer can be verified in polynomial time is called NP. Assume there exists an algorithm that generates a solution for the train synchronization timetabling problem. Determining whether the solution is feasible for the train synchronization timetabling problem implies several steps. Constraints (3) and (4) track the arrival time and the departure time. Constraints (5) and (13) limit running time, dwell

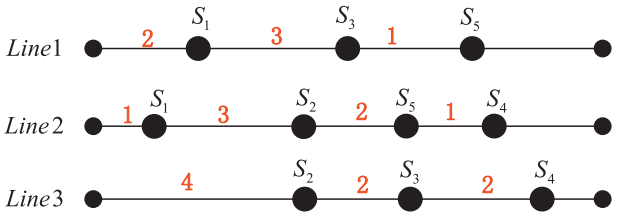


**Fig. 21.** Basic parameters for setting up polynomial reduction.

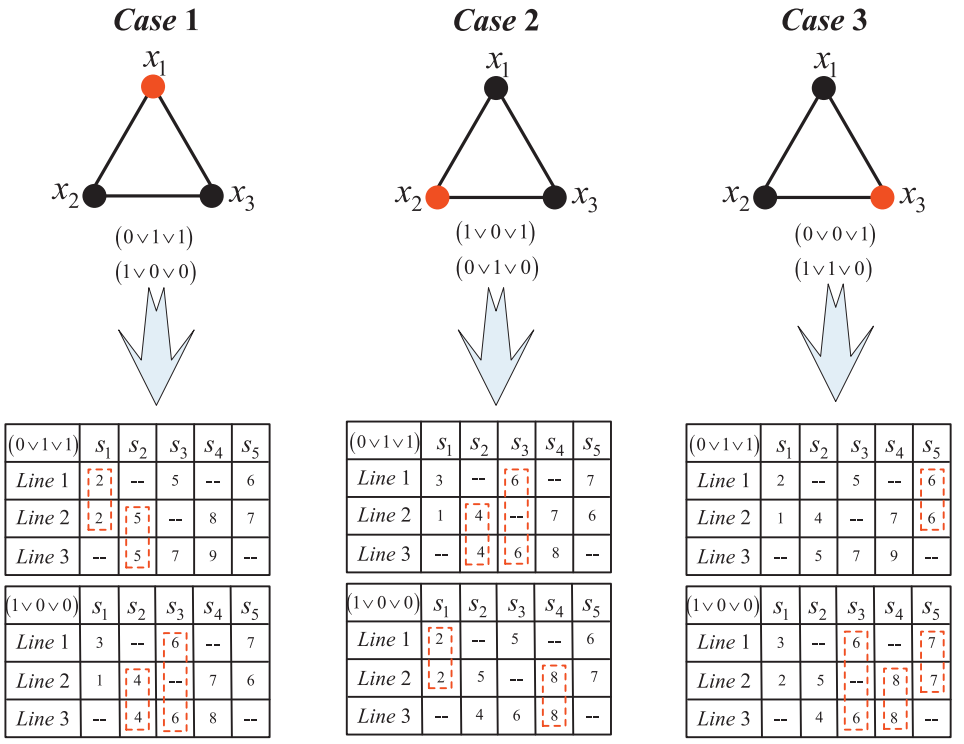


| (0∨1∨1) | $s_1$ | $s_2$ | $s_3$ | $s_4$ | $s_5$ |
|---|---|---|---|---|---|
| Line 1 | 2 | -- | 5 | -- | 6 |
| Line 2 | 2 | 5 | -- | 8 | 7 |
| Line 3 | -- | 5 | 7 | 9 | -- |

| (1∨0∨0) | $s_1$ | $s_2$ | $s_3$ | $s_4$ | $s_5$ |
|---|---|---|---|---|---|
| Line 1 | 3 | -- | 6 | -- | 7 |
| Line 2 | 1 | 4 | -- | 7 | 6 |
| Line 3 | -- | 4 | 6 | 8 | -- |

| (1∨0∨1) | $s_1$ | $s_2$ | $s_3$ | $s_4$ | $s_5$ |
|---|---|---|---|---|---|
| Line 1 | 3 | -- | 6 | -- | 7 |
| Line 2 | 1 | 4 | -- | 7 | 6 |
| Line 3 | -- | 4 | 6 | 8 | -- |

| (1∨0∨0) | $s_1$ | $s_2$ | $s_3$ | $s_4$ | $s_5$ |
|---|---|---|---|---|---|
| Line 1 | 2 | -- | 5 | -- | 6 |
| Line 2 | 2 | 5 | -- | 8 | 7 |
| Line 3 | -- | 4 | 6 | 8 | -- |

| (0∨1∨1) | $s_1$ | $s_2$ | $s_3$ | $s_4$ | $s_5$ |
|---|---|---|---|---|---|
| Line 1 | 2 | -- | 5 | -- | 6 |
| Line 2 | 1 | 4 | -- | 7 | 6 |
| Line 3 | -- | 5 | 7 | 9 | -- |

| (1∨0∨0) | $s_1$ | $s_2$ | $s_3$ | $s_4$ | $s_5$ |
|---|---|---|---|---|---|
| Line 1 | 3 | -- | 6 | -- | 7 |
| Line 2 | 2 | 5 | -- | 8 | 7 |
| Line 3 | -- | 4 | 6 | 8 | -- |

**Fig. 22.** Values for true clauses with three different literals in NAE-3SAT.

time, departure time and headway to ensure operational safety. Constraint (14) ensures attendance to increase income. Constraints (15) and (16) are utilized to calculate the synchronization events. The last step is to make a comparison with $K$. In conclusion, we need a polynomial time to demonstrate the feasibility of solutions, i.e., the train synchronization timetabling problem belongs to NP.

(2) The second step is to prove the problem $P$ can be reducible to problem $Q$.

We present a specific experiment of the train synchronization timetabling problem which can be the reduction from NAE-3SAT with $|C|$ clauses. Setting three lines with $|X|=3$(see Fig. 21), lines in problem $Q$ correspond to literals $X=\{x_1, x_2, x_3\}$ in problem $P$. There are five transfer stations labeled as $\{s_1, s_2 \ldots s_5\}$ and $S(l_1)\cap S(l_2)=(s_1, s_5)$, $S(l_2)\cap S(l_3)=(s_2, s_4)$, $S(l_1)\cap S(l_3)=s_3$.

The planning period is $[T_1, T_2]=[0, 10]$. The upper and lower bounds of running times and dwell times for all lines are zero, i.e., the train will operate strictly according to the set schedules. The upper and lower bounds of headways are zero and one. The synchronization time windows are set to zero, i.e., the successful synchronization occurs when trains arrive simultaneously at the transfer station. The all transfer walking times $t^T_{ll's}=0$ and the departure time of the first trains at any stations would be not earlier than zero and not later than $T_2$, transfer passenger matrix $P^H_{lql'q's}(t)$ for all directions are set to one person, i.e., all transfer synchronization events are equally important in this network. Table 10 describes the precise departure times at all transfer stations in different lines.

If clause $C_i=(x_1\vee x_2\vee x_3)$, choosing $x_1=t^D_{111}=0$, $x_2=t^D_{211}=1$, and $x_3=t^D_{311}=1$. In Fig. 22, Case 1 represents line 1, line 2 and line 3 with departure times of 0, 1 and 1 respectively. We use red dotted circles to highlight successful synchronizations which imply that two trains arrive simultaneously at transfer stations $s_1$ and $s_2$. The successful transfer events also show a true clause. The same is true with (1, 0, 0) in case 1. In cases 2 and 3, variables $x_2$ and $x_3$ have different values with the others, however, they get true clauses with three literals. Let there be $\tilde{m}$ clauses, this reduction sets up $2\times\tilde{m}$ synchronization events.

**Table 10**
Departure times at all transfer stations, represented by the symbol.

| Station | $S_1$ | $S_2$ | $S_3$ | $S_4$ | $S_5$ |
|---|---|---|---|---|---|
| Line 1 | $t^D_{111}+2$ | – | $t^D_{111}+5$ | – | $t^D_{111}+6$ |
| Line 2 | $t^D_{211}+1$ | $t^D_{211}+4$ | – | $t^D_{211}+7$ | $t^D_{211}+6$ |
| Line 3 | – | $t^D_{311}+4$ | $t^D_{311}+6$ | $t^D_{311}+8$ | – |

If clause $C_i=(x_1\vee x_2)$, we could easily obtain the successful synchronizations in this problem which represents a true clause. Similarly, $C_i=(x_1\vee x_3)$ and $C_i=(x_2\vee x_3)$ are true as well.

In consequence, we define $K=2\times\bar{m}+\bar{n}$ in this train synchronization timetabling problem, where $\bar{m}$ is the number of clauses with three different literals, and $\bar{n}$ is for two. Thus, the polynomial reduction from NAE-3SAT to the train synchronization timetabling problem can be done in polynomial time. Achieving through the above sufficient steps, where its decision version belongs to NP-complete, and the optimization problem belongs to NP-hardness.

## References


Albrecht, T., Oettich, S., 2002. A new integrated approach to dynamic schedule synchronization and energy-saving train control. WIT Trans. Built Environ. 61.

Castelli, L., Pesenti, R., Ukovich, W., 2004. Scheduling multimodal transportation systems. Eur. J. Operat. Res. 155 (3), 603–615.

Ceder, A., Golany, B., Tal, O., 2001. Creating bus timetables with maximal synchronization. Trans. Res. Part A 35 (00), 913–928.

Ceder, A., 2007. Public Transit Planning and Operation: Theory Modeling and Practice. Elsevier, Butterworth-Heinemann.

Ceder, A.A., Hassold, S., Dano, B., 2013. Approaching even-load and even-headway transit timetables using different bus sizes. Public Transport 5 (3), 193–217.

Cevallos, F., Zhao, F., 2006. Minimizing transfer times in public transit network with genetic algorithm. Trans. Res. Record 1971 (1), 74–79.

Chang, Y.H., Yeh, C.H., Shen, C.C., 2000. A multi-objective model for passenger train services planning: application to Taiwan's high-speed rail line. Transp. Res. Part B: Method. 34 (2), 91–106.

Chakroborty, P., 2003. Genetic algorithms for optimal urban transit network design. Comput.-Aided Civ. Infrastruct. Eng. 18 (3), 184–200.

Daduna, J.R., Voß, S., 1995. Practical experiences in schedule synchronization. Lect. Notes Econ. Math. Syst. Comput.-Aided Transit Schedul. 39–55.

Desaulniers, G., Hickman, M.D., 2007. Public transit. Handbooks Operat. Res. Manage. Sci. 14, 69–127.

Domschke, W., 1989. Schedule synchronization for public transit networks. Operation Research Spectrum 11 (1), 17–24.

Dou, X., Meng, Q., Guo, X., 2015. Bus schedule coordination for the last train service in an intermodal bus-and-train transport network. Trans. Res. Part C 60, 360–376.

Eranki, A., 2004. A Model to Create Bus Timetables to Attain Maximum Synchronization Considering Waiting Times at Transfer Stops Master's Thesis. University of South Florida.

Fleurent, C., Lessard, R., Séguin, L., 2004. Transit timetable synchronization: evaluation and optimization. In: Proceedings of the 9th International Conference on Computer-Aided Scheduling of Public Transport. San Diego, pp. 9–11.

Gallo, M., Montella, B., D'Acierno, L., 2011. The transit network design problem with elastic demand and internalization of external costs: an application to rail frequency optimization. Trans. Res. Part C 19 (6), 1276–1305.

Guihaire, V., Hao, J.K., 2008. Transit network design and scheduling: a global review. Trans. Res. Part A 42 (10), 1251–1273.

Guo, X., Wu, J., Sun, H., Liu, R., Gao, Z., 2016. Timetable coordination of first trains in urban railway network: a case study of beijing. Appl. Math. Modell. 40 (17-18), 8048–8066.

Hao, L., Zhang, X., 2000. Study on equilibrium evaluation of train flow arrived at and departure from a station. J. China Railway Soc. 22 (5), 13–16.

Ibarra-Rojas, O.J., Rios-Solis, Y., 2012. Synchronization of bus timetabling. Trans. Res. Part B 46 (5), 599–614.

Ibarra-Rojas, O.J., Delgado, F., Giesen, R., Muñoz, J.C., 2015a. Planning, operation, and control of bus transport systems: A literature review. Trans. Res. Part A 77, 38–75.

Ibarra-Rojas, O.J., López-Irarragorri, F., Rios-Solis, Y.A., 2015b. Multiperiod bus timetabling. Trans. Sci. 50 (3), 805–822.

Ibarra-Rojas, O.J., Lopez-Irarragorri, F., Rios-Solis, Y.A., 2016. Multiperiod bus timetabling. Transp. Sci. 50 (3), 805–822.

Idoumghar, L., Melkemi, M., Schott, R., Aouad, M.I., 2011. Hybrid PSO-SA type algorithms for multimodal function optimization and reducing energy consumption in embedded systems. Appl. Comput. Intell. Soft Comput. 2011 (3), 1–12.

Kang, J.E., Chow, J.Y., Recker, W.W., 2013. On activity-based network design problems. Trans. Res. Part A 57, 398–418.

Kang, J.E., Chen, A., 2016. Constructing the feasible space-time region of the household activity pattern problem. Trans A 1–32.

Kang, L., Wu, J., Sun, H., Zhu, X., Gao, Z., 2015a. A case study on the coordination of last trains for the Beijing subway network. Trans. Res. Part A 72, 112–127.

Kang, L., Wu, J., Sun, H., Zhu, X., Wang, B., 2015b. A practical model for last train rescheduling with train delay in urban railway transit networks. Omega 50, 29–42.

Kou, C.G., He, S.W., He, B.S., 2014. Study on connection optimization of last train departure time on urban mass transit network. Adv. Mater. Res. 1030, 2211–2214.

Liebchen, C., 2008. The first optimized railway timetable in practice. Trans. Sci. 42 (4), 420–435.

Lin, C.C., Chen, S.H., 2008. An integral constrained generalized hub-and-spoke network design problem. Transp. Res. Part E: Logist. Transp. Rev. 44 (6), 986–1003.

Mesa, J.A., Ortega, F.A., Pozo, M.A., 2014. Locating optimal timetables and vehicle schedules in a transit line. Ann. Operat. Res. 222 (1), 439–455.

Nachtigall, K., Voget, S., 1997. Minimizing waiting times in integrated fixed interval timetables by upgrading railway tracks. Eur. J. Operat. Res. 103 (3), 610–627.

Niknam, T., Amiri, B., Olamaei, J., Arefi, A., 2009. An efficient hybrid evolutionary optimization algorithm based on PSO and SA for clustering. J. Zhejiang Univ. Sci. A 10 (4), 512–519.

Niu, H., Tian, X., Zhou, X., 2015. Demand-driven train schedule synchronization for high-speed rail lines. IEEE Trans. Intell. Trans. Syst. 16 (5), 2642–2652.

Odijk, M.A., 1996. A constraint generation algorithm for the construction of periodic railway timetables. Trans. Res. Part B 30 (6), 455–464.

Palma, A.D., Lindsey, P., 2001. Optimal timetables for public transportation. Trans. Res. Part B 35 (8), 789–813.

Wong, R.C.W., Leung, J.M., 2004. Timetable synchronization for mass transit railway. In: Proceedings of the 9th International Conference on Computer-Aided Scheduling of Public Transport.

Wong, R.C., Yuen, T.W.Y., Fung, K.W., Leung, J.M., 2008. Optimizing timetable synchronization for rail mass transit. Trans. Sci. 42 (1), 57–69.

Wu, Y., Yang, H., Tang, J., Yu, Y., 2016. Multi-objective re-synchronizing of bus timetable: model, complexity and solution. Trans. Res. Part C 67, 149–168.

Wu, J., Liu, M., Sun, H., Li, T., Gao, Z., Wang, D.Z., 2015. Equity-based timetable synchronization optimization in urban subway network. Trans. Res. Part C. 51, 1–18.
Salicrú, M., Fleurent, C., Armengol, J.M., 2011. Timetable-based operation in urban transport: run-time optimization and improvements in the operating process. Trans. Res. Part A 45 (8), 721–740.
Sels, P., Dewilde, T., Cattrysse, D., Vansteenwegen, P., 2016. Reducing the passenger travel time in practice by the automated construction of a robust railway timetable. Trans. Res. Part B 84, 124–156.
Shafahi, Y., Khani, A., 2010. A practical model for transfer optimization in a transit network: model formulations and solutions. Trans. Res. Part A 44 (6), 377–389.
Shi, Y., Eberhart, R.C., 1999. Empirical study of particle swarm optimization. Evolutionary computation, CEC 99. In: Proceedings of the 1999 Congress on. IEEE Transactions on Intelligent Transportation Systems 3.
Tong, L., Zhou, X., Miller, H.J., 2015. Transportation network design for maximizing space–time accessibility. Trans. Res. Part B 81, 555–576.
Vaughan, R., 1986. Optimum polar networks for an urban bus system with a many-to-many travel demand. Trans. Res. Part b 20 (3), 215–224.
Yan, S., Chen, H.L., 2002. A scheduling model and a solution algorithm for inter-city bus carriers. Trans. Res. Part A 36 (9), 805–825.
Yang, X., Li, X., Gao, Z., Wang, H., Tang, T., 2013. A cooperative scheduling model for timetable optimization in subway systems. IEEE Trans. Intell. Trans. Syst. 14 (1), 438–447.
Yang, X., Ning, B., Li, X., Tang, T., 2014. A two-objective timetable optimization model in subway systems. IEEE Trans. Intell. Trans. Syst. 15 (5), 1913–1921.
Yang, X., Chen, A., Li, X., Ning, B., Tang, T., 2015. An energy-efficient scheduling approach to improve the utilization of regenerative energy for metro systems. Trans. Res. Part C 57, 13–29.
Yang, X., Chen, A., Ning, B., Tang, T., 2016. A stochastic model for the integrated optimization on metro timetable and speed profile with uncertain train mass. Trans. Res. Part B 91, 424–445.
Zhou, W., Deng, L., Xie, M., Yang, X., 2013. Coordination optimization of the first and last trains' departure time on urban rail transit network. Adv. Mech. Eng. 5 (3) 848292.
Zhu, J., 2009. A modified particle swarm optimization algorithm. J. Comput. 4 (12), 1231–1236.